(NASA-TM-86045) MODELS OF THE HARD X-RAY SPECTRUM OF AM HERCULIS AND IMPLICATIONS FOR THE ACCRETION RATE (NASA) 40 p HC A03/MF A01 CSCL 03A

N84-18123

Unclas
G3/89 18255

NASA

Technical Memorandum 86045

MODELS OF THE HARD X-RAY SPECTRUM OF AM HERCULIS AND IMPLICATIONS FOR THE ACCRETION RATE

J.H. Swank,
A.C. Fabian, and
R.R. Ross

December 1983

National Aeronautics and
Space Administration

Goddard Space Flight Center
Greenbelt, Maryland 20771

MODELS OF THE HARD X-RAY SPECTRUM OF AM HERCULIS AND IMPLICATIONS FOR THE ACCRETION RATE

J.H. Swank[1,2], A.C. Fabian[2], and R.R. Ross[3]

[1]Laboratory for High Energy Astrophysics
NASA/Goddard Space Flight Center
Greenbelt, Maryland 20771

[2]Institute of Astronomy
Madingley Road
Cambridge CB3 OHA, England

[3]Physics Department
College of the Holy Cross
Worcester, Massachusetts 01610

ABSTRACT

Phenomenological fits to the hard X-ray spectrum of AM Herculis left unexplained the high equivalent width (0.8 ± 0.1 keV) of Fe Kα emission. A purely thermal origin implies a much steeper spectrum than was observed. We have investigated with Monte Carlo calculations scattering and fluorescent line production in a cold or partially ionized accretion column of hard X-rays emitted at the base. The strength of the iron emission and the flat spectral continuum can be explained by the effects of fluorescence and absorption within the accretion column and the surface of the white dwarf on a thermal

X-ray spectrum. Thomson optical depths across the column in the range 0.2 - 0.7 are acceptable. The accretion rate and gravitational power can be deduced from the optical depth across the column, if the column size is known, and, together with the observed hard X-ray and polarized light luminosities, imply a lower limit for the luminosity in the UV to soft X-ray range, for which the observations give model-dependent values. Estimates of the column size differ by a factor of 40. Small spot sizes and low luminosities would be consistent with the soft component being the expected reprocessed bremsstrahlung and cyclotron radiation, although the constraint of matching the spectrum confines us to solutions with fluxes exceeding 20% the Eddington limit, for which our approximations may not hold. The larger spot sizes are consistent with our fit to the spectrum, but a mechanism would be needed to enhance the soft component luminosity at the expense of the hard X-rays.

I. INTRODUCTION

The hard X-ray spectra of AM Herculis includes strong Fe emission (Rothschild et al. 1981; Pravdo 1979). The equivalent widths obtained in model fits for several detectors and observations (0.5-1.0 keV) were all too high to be explained as thermal emission by gas as hot as the lower limit of 26 keV needed to fit the high energy continuum and there was no evidence within the models tried, for gas of cooler temperatures. Rothschild et al. deduced from the X-ray light curves and optical polarization measurements that the emission region must not extend more than ~ 1% of the white dwarf radius above the surface and should cover ~ 2 x 10^{-3} of the surface. These values correspond to an accretion column radius ~ 10% of the white dwarf radius. This picture suggested that the albedo of the white dwarf could observably affect the spectrum. The idea allowed a better fit to the continuum over the extended energy range, but it did not explain the strength of the Fe emission as long as the abundances (of the freshly accreted material) were near solar. Calculations by Bai (1979) and Basko (1978) imply an equivalent width of $\lesssim$ 0.3 keV. Thus while an assumed bremsstrahlung emission spectrum, an albedo enhancement of the hard X-rays, an absorbing column and line emission gave an acceptable phenomenological fit to the data, the amount of line emission was unexplained and the absorption by column material was not required to be consistent with the accretion rate and the viewing angle.

Spectra for spherical accretion onto non-magnetic white dwarfs have been calculated by Kylafis and Lamb (1979;1982) for the possible accretion rates and white dwarf masses, assuming that the accreting material is completely ionized behind the shock that is formed. They calculated the flow, the structure of the shock region, the bremsstrahlung of the hard X-rays and reprocessing of these in the white dwarf and the inflowing material. They used Monte Carlo calculations to determine the spectra for a given flow structure and took the effects on the structure into account iteratively. The resulting spectra are significantly steeper than the data from AM Her at energies below ~ 15 keV and the Fe emission feature is not addressed. Kylafis (1978) and Ross and Fabian (1980) agreed that heavy elements in the inflowing material should produce significant absorption edges, although their different approaches and quantitative results disagree. For accretion in a column, more photons will escape without being either down-scattered in energy or absorbed, so that detailed agreement between the AM Her data and any of the spherically symmetric calculations is not expected.

If the geometry of an accretion column, a shock close to the white dwarf surface and a spectrum generated in the shock region are assumed, the observed spectrum can be calculated. In this paper we show that only for a restricted range of column parameters can any emission spectrum agree with the observations and further, that some aspects of the emission spectrum are also prescribed. We wish to address the following questions: (1) Can the Fe emission be explained without postulating that the Fe abundance is enhanced? (2) Can geometric effects, namely the presence of the column, increase the equivalent width by maintaining a large solid angle of fluorescing material, yet keeping a low transverse opacity to allow the fluoresced line and the lower energy flux to escape? (3) Can the Fe emission be used as an indicator of the conditions in the emission region and give independent information about the accretion rate? The luminosity of the component which is seen in the 1/4 keV X-rays and how it arises have been at issue (Raymond et al. 1979; Fabbiano et al. 1981; Kylafis and Lamb 1979, 1982; King and Lasota 1979; Frank, King and Lasota 1982; Kuijpers and Pringle 1982; King 1982). An independent approach to estimate the gravitational power would be useful.

We assume a flat hard X-ray emission region at the bottom of the accretion funnel. A Monte Carlo calculation gives the emergent spectrum, angular distribution and distribution up the column of photons of a given energy > 1 keV. We then ask whether for given choices of the density at the base of the column (just above the shock), the radius of the column and the radius of the white dwarf, there is some choice of input spectrum which can match the data. Finally we ask whether such a spectrum is consistent with being produced in the accretion indicated by the column parameters. We do not follow the fate of photons absorbed and reemitted below 1 keV. For our purposes they are absorbed. The models we tried are detailed in Section II. Section III describes the equivalent widths and continua generated for a range of column parameters and emission spectra. The implications of the restricted parameter ranges that fit the data are discussed in Section IV. Our conclusions are summarized in Section V.

After this work was completed, we found that Imamura and Durisen (1983) have calculated spectra for a totally ionized accretion column. Our approaches differ, but some of the results such as the qualitative behavior of the angular dependence, are the same, independent of the different assumptions about the ionization above the shock and the spectrum produced in the emission region. However the emergent spectra are crucially dependent on these differences and the competition of cooling mechanisms also depends on them.

II. MODELS

We investigated a variety of situations, but in all we assumed a "pill box" shaped high temperature emission region at the base of a cylindrical column as shown in Figure 1. In all the Monte Carlo calculations the height was assumed infinitesimal. We discuss below the effect of a finite shock height (h in Fig. 1). Photons were created uniformly over the base and isotropic in direction. For a stellar radius R and height z above it we usually took the density to fall as $(R+z)^{-3/2}$, as for spherical infall (neglecting radiation pressure). The $(R+z)^{-5/2}$ dependence that collimation by an undistorted dipole field would imply did not produce significantly different results. Radiation pressure should not appreciably alter the flow unless the flux in the soft component approaches the Eddington limit. Imamura and Durisen (1983) found effects of a few percent in their calculations. Mean free paths for a total cross section for absorption or scattering were chosen and each photon was tested for having escaped the column or white dwarf and for crossing the column-white dwarf boundary. A photon not escaping was scattered or absorbed and above the threshold of 7.1 keV a further choice allowed it to fluoresce a 6.4 keV photon with probability 0.34 (Hatchett, Buff and McCray 1976), if absorbed by Fe. The scattering angle θ was distributed as $1+\cos^2\theta$ and the energy of the photon changed from E to $E/(1 + (1 - \cos\theta)E/m_ec^2)$. Calculations were done for a grid of energy bins and when the photon moved across a bin boundary the cross sections were changed to those of the new bin center. Results for albedo alone were compared to those of Bai and Ramaty (1978) for the sun for 30 keV and 20 keV bremsstrahlung, with deviations of ~ 10% attributable to the coarseness of our energy grid. The equivalent widths and general shape of the continuum were insensitive to such effects, however.

We used the photoionization cross sections for neutral elements (Storm and Israel 1967), but assumed H and He fully ionized by the soft X-ray source. For the higher Z elements we used the "solar" abundances chosen by Fireman (1974). In particular that of Fe is 4×10^{-5} of H by number, which Fireman took as an average of Withbroe's preferred values for the solar photospheric and coronal measurements (Withbroe 1971), and which has been substantiated by more recent work (Blackwell and Shallis 1979). It is unlikely that the abundance of Fe is as much as twice the value we adopt (Pagel and Edmunds 1981).

We considered the contributions of the elements C through Ni in 3 groups according to the K-shell ionization energy: (1) C, O, Ne, (2) Mg, Si, and S and (3) Ar, Ca, Fe and Ni, except that the Fe L shell contribution was included with the first group. A simple allowance for the effects of photoionization could then be made by adjusting a fraction of the elements' contributions to the effective cross section. We discuss below results for the column material being "cold", i.e. with no ionization assumed for $Z > 2$, and "partially ionized", that is, with part of higher Z elements stripped just above the shock. Close enough to the emission region for optically thin conditions to apply, the elements in the 3 groups should be stripped for $\xi_X \gtrsim 10^2$, 10^3 and 3×10^3, respectively, where $\xi_X = \frac{L}{nz^2}$ for a point source luminosity L at a distance z, a density n and a 15 keV exponential spectrum (Hatchett, Buff and McCray 1976). For a non-point source the quantity corresponding to ξ_X is $4\pi cU/n$, where U is the radiation energy density and c the velocity of light. For a 3×10^5 K blackbody flux of 10^{34}-$10^{34.5}$ ergs s^{-1} and a 30 keV bremsstrahlung flux of $10^{32.5}$ ergs s^{-1}, which might better represent the AM Her case, we found using G. Ferland's photoionization program (Ferland and Truran 1980,1981) that the critical range of the bremsstrahlung ξ_X for an infinite half space was 20-40 for fully ionized O to go from 1% to > 50%. Trapping of radiation may decrease the required values of ξ_X somewhat. Along the axis of the column, at height $z > h$ (see Figure 1) the hard X-ray shock region luminosity L_{BR} should give an effective $\xi_X \sim (L_{BR}/n_0 R_c^2)\, \ell n\, (1 + R_c^2/z^2)$ for density n_0 above the shock. With $\tau_\perp = 2\, n_0\, \sigma_T R_c$, column base area $f4\pi R^2$ and $R = 5 \times 10^8\, R_1$ cm, $\xi_X \sim 20$

$(L_{BR}/2 \times 10^{32})$ $(0.3/\tau_{\perp})$ $(2 \times 10^{-3}/f)^{1/2}$ R_1^{-1} $\ell n(1 + R_c^2/z^2)$. For our estimated values of L_{BR}, $\tau_{\perp}$ and f (discussed below), a majority of the O would be stripped at z ~ h. Possible parameter values could give ξ_x ~ 500 over a scale height R_c however. The low energy (0.5-2 keV) output is sensitive to the ionization state in the lower part of the column. The partially ionized model for which we give results below assumed 90% of C, O, Ne and the Fe L shell stripped and 50% of Mg, Si and S in a region of height R_c. These ionization levels should be reasonable upper limits for the pre-shock accreting gas.

While recognizing that heavy elements would be ionized only close to the shock, Imamura and Durisen (1983) argued that because most of the hard X-rays are scattered out of the funnel by the photoionized part just above the shock, a completely ionized funnel should be a reasonable model. We are interested, however, in just those aspects of the problem, the Fe line and the slope of the spectrum, which are sensitive to this difference.

We also calculated results for a completely ionized column with $\tau_{\perp}$ up to ~ 7. The number of scatterings is then large for most photons and the spectrum steepened at high energies as in the spherical accretion calculated by Kylafis and Lamb (1982) and the funnel accretion calculated by Imamura and Durisen (1983). However the spectrum rises much more steeply below ~ 6 keV than do the data. This is still true for the funnel accretion, even though the steepening is less severe than for the spherically symmetric case (Imamura and Durisen 1983).

For low accretion rates shocks are expected to be higher above the white dwarf surface and we can expect to "see" the sides of the shock region. The ratio of radiation escaping out the sides to that entering the column or the white dwarf should be $\lesssim h/R_c$, where

$$h/R_c \sim 1/2(h/R)f^{-1/2} \sim 0.1\ (h/0.01R)\ (2 \times 10^{-3}/f)^{1/2}. \qquad (1)$$

We considered the effect of such a contribution approximately by adding a fraction of unaltered emission spectrum.

Rothschild et al. (1981) concluded that when a Gaunt factor was included, and albedo enhancement of high energies allowed for, the high energy fall-off was like that of a 30^{+10}_{-5} keV thermal bremsstrahlung spectrum. We found that, indeed, for a wide range of column models a component with kT ~ 30 keV was needed to give the behavior above ~ 10 keV. 100 keV was qualitatively too hard and 20 keV too steep. Thus at high energies the phenomenological model approximated fairly well the situation we assume here. As a first approximate emission region spectrum we took 30 keV bremsstrahlung with a Gaunt factor ($\alpha\ E^{-0.3}$) and a 0.1 keV equivalent width line at 6.9 keV. However the emission region in which the shocked gas cools is expected to have a temperature distribution in which the cooler denser gas gives a high differential emission measure. Furthermore, the cooling time ($2 \times 10^{11} T^{1/2} n^{-1} s$) exceeds the recombination time for Fe (~ $10^{12}\ n^{-1}s$) so that Fe in several keV gas should contribute 6.7 and 6.9 keV lines. The continua produced at these temperatures are ineffectual in producing a fluorescent Fe line. The amount of lower temperature gas which can be compatible with the observations depends on the assumed ionization conditions, since the contribution to the observed continuum can be masked by absorption.

To study the effect of lower temperature contributions, it seemed adequate to represent them by a thermal component with kT = 5 keV and an associated emission line at 6.7 keV with an equivalent width of 1.5 keV. Comparison showed that spectra output from spherically symmetric shock calculations in which Compton cooling by a specified soft component was included could be approximated by our 2 temperature simplification. The latter is more general, if we do not assume a theory of the production. However, it is important that it could approximate spectra theoretically expected, even if spherically symmetric calculations are not exactly appropriate. For the low shock height implied by the observations we expected the spherically symmetric calculations to be reasonable estimates and this is indeed born out by the results of Imamura and Durisen (1983) for the funnel geometry and the completely ionized column. (The latter assumption would also influence a self-consistent calculation of the structure of the post-shock region.)

We calculated the structure of the postshock regions for spherically symmetric infall as described in Ross and Fabian (1980), except that instead of calculating the blackbody luminosity self-consistently, we calculated results for a grid of assumed blackbody luminosities, in order to allow for its possible enhancement, by nuclear burning, for example. Results generated for those values which are produced in a self-consistent calculation agreed with the latter. Radiation pressure effects were neglected as unimportant at low accretion rates and luminosities. As in Kylafis and Lamb (1979) the ratio of energy density to flux was taken to be constant, while in Kylafis and Lamb (1982) a more accurate estimate was used. The shock stand-off distances we obtained in the self-consistent calculations agreed, as they should, with those tabulated in Kylafis and Lamb (1982) for low accretion rates. At accretion rates 10% of the Eddington limit, the correction gives shock heights lower by a factor of about 2.

The spectra emitted in the Compton cooled shock regions were calculated including the thermal line emission expected according to the models by Raymond and Smith (1977; 1979). (Pravdo and Smith 1979 give a table of the equivalent width of the 6.7-6.9 keV Fe XXIV and Fe XXV complex as a function of temperature for [Fe/H] = 2.5 x 10^{-5}.)

In summary, the models for which results are given in Section IV are (1) a cold column with 30 keV bremsstrahlung emission spectrum, (2) a partially ionized column for 30 keV, (3) the same as (1) or (2) with addition of 10% of the emission spectrum, (4a) a partially ionized column with 30 keV plus 5 keV (number spectrum α $E^{-1.3}$ exp(-E/30) + X $E^{-1.4}$ exp(-E/5)), and (4b) cold and partially ionized columns with emission spectra from spherically symmetric shock models.

III. RESULTS

Both the equivalent widths and continua depend on the optical depth across the column and are insensitive to different choices of n_0, R_c and R for given $\tau_\perp$. The total equivalent width of the fluorescent and thermal components is shown in Figure 2. As might be expected, for models (1) and (2), the fluorescent equivalent width increases with $\tau_\perp$. The column effectively gives an albedo similar to that from the white dwarf. For a given $\tau_\perp$ the partially ionized lower column gives a higher equivalent width. The value shown for $\tau_\perp$ = 0.01 is that for the albedo diluted by the source seen directly, equivalent to the optically thin column for a very low accretion rate.

The band shown for AM Her is for the best HEAO 1 A-2 xenon detector measurement (0.84 ± 0.09 keV), which agreed with all the others from similar detectors. For the argon detector the equivalent width of a single line was more model dependent (0.53 ± 0.09 versus 0.7 keV), although its energy range and channel resolution should make it more sensitive to faults in the models. The requisite large total equivalent width cannot be obtained from fluorescence alone unless $\tau_\perp \gtrsim 1$. Then, as Figure 3c shows, the continua are flatter or harder than the data and the absorption edge due to Fe too deep. (The data give a 90% upper limit of 0.7 to an increment in optical depth at 7.1 keV). Figure 2 indicates those models for which the continuum fit was adequate. For an emission spectrum of such high temperature that the associated thermal line emission is small and conditions such that the continuum fits the data, the equivalent width of the emission feature (due to fluorescence) is too low.

In Figure 3 the observed spectrum is drawn down to 0.5 keV. The HEAO 2 Solid State Spectrometer measurements (Swank and Szkody 1984) indicate that the low energy turnover represented in the fits to data above 2 keV by absorption does not extrapolate as $\exp(-N_H\sigma(E))$. We can expect the true ionization state of the column to be somewhere between the cases in our models 1 and 2, so spectra which are too steep with the cold column or too flat with our partially ionized model we regard as unacceptable.

If a spectrum is too flat, but has a large fluorescent line emission it can be diluted by some unabsorbed emission even if the latter does not contain a thermal line flux. It is possible to get fits with such models for high $\tau_\perp$, although the constraint of large enough equivalent width forces the Fe edge to be about at the 90% upper limit. It is not quite possible to rule out such solutions on the grounds that the observed line centroid has not been shifted down by more than ~ 0.2 keV, because with the column geometry the average number of scatterings by escaping line photons is still $\lesssim 1$ for $\tau_\perp \sim 3$ if the column is cold or only partially ionized. It is possible to rule out a very thick fully ionized column because the line photons scatter more than twice before leaving.

If low temperature emission is included, total equivalent widths of 0.7-0.8 keV can be obtained for $\tau_\perp$ in the range 0.2-0.7, without generating an unacceptable low energy excess. A range of spectra are shown in Figure 3b which are within the uncertainties of the incident spectrum inferred from the data. Spherical shock models with Compton cooling by a low temperature (20-50 eV) blackbody component of $L_{BB} \sim 10^{37}$ ergs s^{-1} (corresponding to $fL_{BB} \sim 2 \times 10^{34}$ ergs s^{-1}) are practically indistinguishable in shape. Figure 3b includes some results for higher L_{BB} for which the spectra are still reasonably in agreement with the data and the predicted hard X-ray luminosity not very much larger than observed. We discuss in Section IV.B, however, the difficulty of matching both the flux and the spectral shape in such a model. In these models most of the flux came from very close to the shock ((z-h)/R $\lesssim$ 0.01), so that the results are consistent with the low height of the apparent emission region. The ratio h/R could be considerably smaller than 0.01. Then the sides of the pillbox would give a negligable further contribution.

Is there a lower limit on the $\tau_\perp$ that are acceptable? We can use the cold column results to put upper limits on how much low temperature component can be included. As $\tau_\perp$ is reduced below 0.2 the amount of low temperature component needed to produce the equivalent width by thermal emission exceeds the allowed limits (see Figure 3a). (The proportional counter measurements of an absorption edge are not as restrictive. The 90 percent lower limit on a jump in τ at 7.1 keV is ~ 0.05).

For $\tau_\perp$ higher than 0.7, the amount of low temperature component required in the emitted spectrum to keep the continuum from being too flat is so great that too much Fe line emission results. If now a contribution of unabsorbed flux escaping the walls of the shock region is included, it is possible that for $\tau_\perp$ somewhat higher than 0.7 the amount of low temperature emission and the fraction of flux viewed directly could be adjusted to give a good fit to the entire spectrum. For $\tau_\perp$ as high as 1.75, however, the Fe K absorption edge is deeper than the limits from the data. We have not extensively explored the loci of parameters giving acceptable fits for the upper limits to $\tau_\perp$. A more detailed study of such solutions seems outside the scope of our approximations.

In Figure 2 the ratio of contributions of the thermal to fluorescent components of the emission feature are also shown. The approximately equal contributions of the acceptable models are allowed by the present proportional counter data. As seen with an energy resolution of 1 keV, the feature appears to have a centroid a few tenths of a keV lower than that in the spectrum of SS Cygni (Swank 1979) measured with the same detector and the same gain, but because of sensitivity to the underlying continuum model, it is not possible to put this in terms of limits on a mixture.

We kept track of the direction in which X-rays escaped. Figure 4a shows the angular dependence of low energy and high energy flux for a cold column. Similar but less extreme results obtained in the partially ionized case. Figure 4b shows that the spectrum would still be harder looking nearly parallel to the column than perpendicular to it and the flux would still be significantly reduced within ~ 30^o of the magnetic axis.

IV. DISCUSSION

A. Accretion rate and Gravitational Power

For accretion onto a white dwarf of mass M we can write the accretion rate as

$$\dot{M} = \tau_\perp \sqrt{f}\, \pi\, \mu_e\, m_p \sigma_t^{-1} \sqrt{2GMR}$$

$$= 4.5\mathrm{x}10^{16}\left(\frac{\tau_\perp}{0.3}\right)\left(\frac{f}{2\mathrm{x}10^{-3}}\right)^{1/2}\left(\frac{M}{M_o}\right)^{1/2} R_1^{\ 1/2}\ \mathrm{gm\ s^{-1}} \qquad (2)$$

and the "gravitational luminosity", $GM\dot{M}/R$ as

$$L_G = 1.2 \times 10^{34} \left(\frac{\tau_\perp}{0.3}\right) \left(\frac{f}{2\times10^{-3}}\right)^{1/2} \left(\frac{M}{M_o}\right)^{3/2} R_1^{-1/2} \text{ ergs s}^{-1}, \qquad (3)$$

corresponding to

$$\frac{L_G}{fL_E} = 0.041 \left(\frac{\tau_\perp}{0.3}\right) \left(\frac{2\times10^{-3}}{f}\right)^{1/2} \left(\frac{M}{M_o}\right)^{1/2} R_1^{-1/2} \qquad (4)$$

where L_E is the Eddington limit for spherically symmetric emission, and μ_e = 1.14. L_G is plotted in Figure 5a against M for the Chandrasekhar mass-radius relation (Chandrasekhar 1957) for $\tau_\perp$ = 0.2, 0.3, and 0.7 with f = 2 x 10^{-3} and for $\tau_\perp$ = 0.3 with f = 2 x 10^{-4}.

The allowed range of L_G in Figure 5a includes between the $\tau_\perp$ = 0.2 and 0.3 lines the gravitational power estimated in Rothschild et al. (1981). Our calculations in fact confirm the basic elements of their phenomenological fit. The albedo effect was reasonably described and the spectrum of photons escaping the column should look like it is absorbed when compared to unabsorbed bremsstrahlung. The method of determining the accretion rate is quite different however, except that in both cases a thin emission region and f ~ 2 x 10^{-3} were assumed. In Rothschild et al. the observed hard X-ray flux was used to deduce an average emission region density assumed to be 4 times the pre-shock density. Here we have deduced from the spectrum what the pre-shock density must be (for given f).

If the gravitational energy of the accreting material is the dominant source of power, L_G should equal the total emitted luminosity ascribable to the accretion at the X-ray emitting pole. What should be taken as the various contributions to this continues to be argued. (See also Heise et al. 1982 and Patterson et al. 1983.) In Table 1 we list the measurement[illegible] [illegible]ill refer to. In Table 2 we give the luminosities based on specified model assumptions.

For the 90% confidence range of blackbody parameters fitted by Tuohy et al. (1978) to typical high state soft X-ray data, $L_s^b \sim 10^{33}$-10^{35} d_{100}^2 ergs s^{-1} was possible. Raymond et al. (1979) found that the UV could be part of the same component if it were a high luminosity 28 eV blackbody. However, the measurements with the Objective Grating Spectrometer (OGS) on HEAO 2 required for a blackbody model kT > 35 eV and $N_H < 6 \times 10^{19}$ cm^{-2} (Heise and Brinkman 1982; Heise et al. 1982). Patterson et al. (1983) emphasize that the N_H determinations of the HEAO 1 and HEAO 2 experiments are inconsistent and the lower N_H of the OGS would imply a relatively small correction for interstellar absorption. The best fit blackbody (kT = 46 eV, $N_H = 3.2 \times 10^{19}$ cm^{-2}) given by Heise et al. (1982) corresponds to 6×10^{32} d_{100}^2 ergs s^{-1}. The soft component spectrum reported by Tuohy et al. (1981) could have corresponded to an even lower luminosity, but as pointed out by those authors, the source varied significantly and the data for that measurement were <u>not</u> representative of the data during the times when the higher energy detectors were collecting it (Rothschild et al. 1981). (Similar variability appears in the HEAO 2 data.) The contradictory values of N_H could be the consequence of the emission not being from an isothermal blackbody. Heise et al. (1982) point out that if the soft X-rays and UV are not components of the same blackbody, a temperature gradient is implied and the spectrum could be significantly affected by radiative transfer in the atmosphere. The bolometric correction is thus very model dependent and in the following we consider the consequences of a range of L_s^b.

Even for L_s^b as small as 6×10^{32} ergs s^{-1} the possible overestimate of L_r is unimportant. Then $L_r + L_u + L_h \sim 3.7 \times 10^{32}$ d_{100}^2 ergs s^{-1}. The estimates for all the components depend on angular distribution models which we know are too simple, but averages over non-eclipse binary phases should be relatively insensitive to this source of error. In Table 2 the luminosities are scaled to the values for a source at 100 pc. This may be a high estimate, as Schmidt, Stockman and Margon (1981) conclude $d = 75^{+25}_{-15}$ pc. In Figure 5a we plot the total emitted luminosity estimates for $L_s^b = 6 \times 10^{32}\ d_{100}^2$ ergs s^{-1} and for $L_{s_2}^b = 2.1 \times 10^{33}\ d_{100}^2$ ergs s^{-1}, each for the range 75-100 pc.

Unless L_s^b is larger than 2×10^{33} ergs s^{-1}, or unless the fraction f for the hard X-ray emission region is smaller than the 2×10^{-3} estimated in Rothschild et al. (1981), L_G exceeds the emitted luminosity for all white dwarf masses above 0.6 M_o. For lower masses the shock temperature would be too low to explain the high energy spectrum. L_G rises as a function of M sufficiently steeply that L_s^b would have to exceed 2×10^{33} ergs s^{-1} by a factor of several. It is not clear whether the bolometric correction and angular dependence can account for so much. L_G is also plotted for $f = 2 \times 10^{-4}$. Clearly, for a spot size much less than 2×10^{-3}, L_G would be consistent with white dwarf masses > 0.6 M_o and with the observed luminosity corresponding to small L_s^b.

A low L_s^b and small spot size would be consistent with each other. If the component is a blackbody viewed at normal incidence,

$$f = 2 \times 10^{-4} \left(\frac{L_s^b}{2 \times 10^{33} \text{ ergs s}^{-1}}\right) \left(\frac{kT}{40 \text{ eV}}\right)^{-4} R_1^{-2}. \qquad (5)$$

Using Eq. (5),

$$L_G = 4.0 \times 10^{33} \left(\frac{L_s^b}{2 \times 10^{33} \text{ ergs s}^{-1}}\right)^{1/2} \left(\frac{kT}{40 \text{ eV}}\right)^{-2} \left(\frac{\tau_\perp}{0.3}\right) \left(\frac{M/M_o}{R_1}\right)^{3/2} . \qquad (6)$$

Figure 5b shows plots of L_G for $\tau_\perp = 0.3$ and d and $L_{s_i}^b$, i = 1, 2, with the solutions for the corresponding total luminosities. Solutions exist for $0.5 < M/M_0 < 1.0$.

Our determination of the gravitational power from the spectrum could thus be consistent either with low soft component luminosity if $f \sim 2 \times 10^{-4}$ - 4×10^{-5} or with soft component luminosity higher than 2×10^{33} ergs s^{-1} if $f \sim 2 \times 10^{-3}$.

The estimate of $f \sim 2 \times 10^{-3}$ (Rothschild et al. 1981) depended on the inclination angle of the orbit(i), the orientation of the magnetic dipole with respect to the rotation axis (θ_m), the hard X-ray eclipse profile, in particular the phase interval $\Delta\phi_L$ of significant obscuration, and an implicit assumption of an unobscured emission cylinder subtending an angle 2α. $\alpha = 2\sqrt{f}$ was the solution of

$$\cos \pi\Delta\phi_L = \cot i \cot \theta_m - \frac{\alpha}{\sin i \sin \theta_m} . \tag{7}$$

The fan beam distribution caused by the accretion column would make the eclipse profile insensitive to disappearance of the far side of the spot over the horizon, that is, to an underestimate of the relevant $\Delta\phi_L$ in Eq. (7). The neglect of this effect by Rothschild et al. should have led to an underestimate of f. Their choices of i and θ_m and recent determinations from low and high state data (Brainerd and Lamb 1983; Barrett and Chanmugam 1984) all differ a little. The differences do not imply more than a factor of 4 in f for given $\Delta\phi_L$ in Eq. (7). However, the differences in i and θ_m do imply uncertainty in the determinations (which have so far neglected the finiteness of the spot size).

B. The Distribution of Power

If the accreting gas forms a high temperature shock, behind which the gas is cooled by cyclotron and bremsstrahlung radiation plus Compton scattering of the flux reprocessed into soft X-ray and UV photons, then these cooling rates should also sum to the gravitational power. In our calculations, the fraction η of the luminosity produced in the emission region which escaped as hard X-rays (> 1 keV) was 0.4-0.5. The implied bremsstrahlung production is then $\lesssim 6.25 \times 10^{32}\ d_{100}^{2}$ ergs s^{-1}. If a similar factor applies to the cyclotron production, the direct cooling would be about $1 \times 10^{33}\ d_{100}^{2}$ ergs s^{-1}. Part of this, $\lesssim 6 \times 10^{32}\ d_{100}^{2}$ ergs s^{-1} would be reprocessed and contribute to Compton cooling of the gas. The exact Compton cooling was not calculated in our model. However, the calculations for spherically symmetric models (Kylafis and Lamb 1982) and for a totally ionized column (Imamura and Durisen 1983) should give upper limits. In their models the contributions ranged from negligable to about equal to the reprocessed flux. For modest accretion rates and $f \sim 10^{-3} - 10^{-4}$, values for the ionized column were $\lesssim 30\%$. Thus the total cooling rate would be $\lesssim 1.3 \times 10^{33}\ d_{100}^{2}$ ergs s^{-1}. From Figure 5b we see that the solutions corresponding to f determined by a soft component of only $6 \times 10^{32}\ d_{100}^{2}$ ergs s^{-1} are approximately consistent for Compton cooling relatively unimportant. For the solutions corresponding to $L_s^b \sim 2 \times 10^{33}\ d_{100}^{2}$ ergs s^{-1}, the total cooling rates deduced are factors of ~ 2 below L_G. Thus if the spot size is correctly indicated by interpreting the soft X-rays as blackbody emission, it is required to be very small for a consistent solution.

There are additional considerations to take into account in evaluating the consistency of possible choices of f and L_s^b. When the spot size is very small, the shape of the emission region may not be thin and flat and a significant fraction of the radiation may be escaping from the sides of the shock region without scattering in the column or the white dwarf. The shock heights of spherically symmetric cases with corresponding accretion luminosities can be interpolated from Table 4 in Kylafis and Lamb (1982) and should be lower limits for the funnel geometry (Imamura and Durisen 1983). For the range of solutions under consideration $0.02 < h/R_c < 0.4$. Figure 2 indicates that a value of 0.1 significantly alters the spectrum. For $h/R_C \gtrsim 0.1$ we were not able to simultaneously fit, for our grid of $\tau_\perp$, (1) the flat continuum, (2) the Fe emission equivalent width and (3) the Fe K absorption edge. As pointed out in Section III, we did not rule out a solution with $\tau_\perp \sim 1.0$. The solutions for $\tau_\perp \sim 0.3$-1.0 (for which $M/M_O \sim 0.6 - 0.8$) have $L_G/fL_E \gtrsim 0.2$, however, so that radiation pressure, which we have neglected could affect the results.

The possibility raised by Tuohy et al. (1978) that the soft component luminosity could be very large led to consideration of nuclear burning of the accreted hydrogen-rich material, since it offered a potentially large luminosity of low energy flux to Compton cool the shock (Katz 1977; Weast et al. 1979; Fabbiano et al. 1981). Our results for the accretion rate could be consistent with an allowed range for steady hydrogen burning (Paczynski and Zytkow 1978; Fujimoto 1982), when scaled to a fraction of the surface. Fig. 5a shows the accretion luminosity, scaled to $f = 2 \times 10^{-3}$, corresponding to the minimum stable burning rate for which the white dwarf has not appreciably expanded (Fujimoto 1982). However the $\sim 2 \times 10^7$ gauss magnetic field of AM Her (Schmidt, Stockman and Margon 1981; Latham, Liebert and Steiner 1981; Young, Schneider and Shectman 1981), while it can confine an accretion shock, cannot confine gas at the densities and temperatures at which it burns (see Fujimoto 1982). Thus the burning accreted material would spread around the white dwarf and not be confined to a spot. Further, the effective rate of accretion would then probably be in the range of unstable burning (Paczynski and Zytkow 1978; Fujimoto 1982; Papaloizou, Pringle and MacDonald 1981; Fujimoto and Truran 1982).

It seems unlikely that Compton cooling by any large extra soft flux is the dominant mechanism for transferring the energy. The energy of the observed Fe emission rules out situations with large optical depths to scattering that would lead to a build up of radiation density in the shock region. Without such a build-up the efficiency is low (Compton cooling ~ 0.05 L_{soft}) for the soft flux to cool the shocked gas and blackbody luminosities at least ~ 10^{38} ergs s^{-1} are needed to leave the low observed hard X-ray luminosity. As Kylafis and Lamb (1982) pointed out, Compton cooling severely steepens the spectrum. (The shock model solutions in Fig. 3b already err in the direction of being too steep.) The white dwarf mass must be high for the spectrum to have a significant high temperature component. Then the implied accretion rates are so high that the shock cannot be Compton-cooled for any blackbody luminosity below the Eddington limit.

We have only investigated uniform steady accretion. Both the soft and hard X-rays are variable (Tuohy et al. 1980; Swank 1979; Heise et al. 1982), and unstable accretion may indicate spatial inhomogeneity as well as non-steady state conditions. An apparently low efficiency for bremsstrahlung, and high ratio of soft to hard luminosity and arguments against nuclear burning have prompted suggestions that the energy could be deposited in the white dwarf atmosphere directly (Frank, King and Lasota 1982; Kuijpers and Pringle 1982), although the specific mechanisms may not work (Lamb 1983). Kuijpers and Pringle have suggested that the protons can be stopped below the white dwarf surface and their energy radiated without formation of a shock. They estimate that instabilities may cause a clumpy distribution across the column with part of the accreting material forming (unstable) shocks at any one time. The hard X-ray emission would then be a function of the fraction of the accretion participating in a shock solution while transfer through all the accreting material would affect the spectrum.

C. 2A0311-227

The spectrum of AM Her is different from that of the other known X-ray bright "polar" or AM Her object 2A0311-227. The spectrum of the latter (White 1981) can be fitted with kT = 18 keV. The Fe feature is of an intensity and energy consistent with thermal emission (see Figure 2). There is no large low energy cutoff indicating non-interstellar absorption except for ~ 0.1 of the orbit during an absorption event which White (1981) interpreted as caused by looking through the accretion column. A lower white dwarf mass or a lower accretion rate would produce a higher shock, so that a larger fraction of the emission may escape the sides of the shock region without having to traverse material above the shock. A higher shock would also imply that albedo from the white dwarf would be less important.

The angular dependence in Figure 4 shows that absorption dips do not require the line of sight to actually pass down the column, although the complete eclipse of the lowest energies in the case of 2A0311-227 (Patterson, Williams and Hiltner 1981) suggests it may occur. For the configuration for AM Her the angle between observer and magnetic axis varies between 40^0 and 90^0. In that case little angular dependence of the uneclipsed flux is to be expected (and the viewing angle cannot be the explanation of the low bremsstrahlung flux). The light curve of 2A0311-227 does not however look like Figure 4c, although it has been supposed that the angle varies between 0^0 and 90^0. The dip occurs during a broader peak of emission. Possibly the maximum angle exceeds 90^0 and part of the emission region is behind the white dwarf during the lower, but unabsorbed part of the light curve.

D. Structure of the Emission Feature

Our prediction that acceptable models of the AM Her spectrum will include significant thermal and fluorescent components could be tested with moderate energy resolution experiments presently possible. The gas scintillation proportional counters, with ~ 10% resolution at 7 keV, on EXOSAT and TENMA could in principle distinguish fluorescent and thermal complexes, although AM Her is a weak source (continuum ~ 0.0013 photons cm^{-2} s^{-1} keV^{-1} at ~ 6.5 keV, total line flux ~ 0.0011 photons cm^{-2} s^{-1}) and the measurements will be background limited. The low background solid state detector and telescope experiment described by Serlemitsos (1982) with 200 eV or 3% resolution at 7 keV would give in a 2000 s observation a better than 20 sigma measure of either component accounting for 1/2 of the total feature. With 200 eV resolution, broadening and energy shifts on the order of 100 eV would also be measurable.

V. CONCLUSIONS

It is clear that the Fe emission equivalent width observed in the spectrum of AM Her can be explained without resorting to an over-abundance of Fe in the accreting material. For sufficient optical depth $\tau_\perp$ across the accretion column equivalent widths of K_α emission can be obtained even larger than the observed 0.8±0.1 keV (Figure 2). When we constrain the model to match the continuum as well, we conclude that probably part of the emission feature is thermal from gas with kT in the range 2-10 keV, but still we require $\tau_\perp \gtrsim 0.2$. The reasons were summarized in Figure 3. For $\tau_\perp$ large enough to give the equivalent width solely through fluorescence excited by ~ 30 keV bremsstrahlung the spectra are too absorbed (Figure 3c). For $\tau_\perp \lesssim 0.2$, so much of the emission feature must have a thermal origin that the continua are too steep (Figure 3a). For $0.2 < \tau < 0.7$ both constraints can be acceptably met (Figure 3b). The mix of temperatures $\lesssim$ 10 keV and as high as 30 keV can be achieved in spherically symmetric shock models, which can be taken to be examples, even if their detailed structure is not correct.

These results imply for a uniform accretion column over a fraction f of the white dwarfs surface a lower limit to the accretion rate and the rate at which gravitational energy needs to be disposed of. For the $f \sim 2 \times 10^{-3}$ implied by the eclipses during the measurement of the hard X-ray spectrum and Chanmugam and Wagner's interpretation of the high state optical polarization, this gravitational luminosity significantly exceeds the hard X-ray and cyclotron luminosity for a white dwarf with $M \gtrsim 0.7\ M_0$. A lower limit on the blackbody luminosity is implied. At least this amount would need to be extracted from the accreting gas. Nuclear burning does not appear to be a viable solution because it would not stay localized below the column. For the $f < 2 \times 10^{-4}$ deduced from interpreting the soft X-rays as the Wien tail of a blackbody viewed at normal incidence with absorption by a minimal interstellar column density, the gravitational luminosity would be consistent with the shock models. The solutions acceptable from this point of view are on the edge of the range of validity of our approach, characterized by relatively high shock heights or high radiation densities. Further theoretical work in several areas seems warranted: (1) the nature of the flow and the spectra for very small spot sizes; (2) the expected spectrum and angular distribution of the soft X-rays; (3) sensitivity to assumptions in the determinations of the orbital and dipole inclinations; (4) accretion regimes in which the flow is unstable; (5) more accurate ionization structure in the accretion column.

Because the emission region must be looked at through the accretion column, fluorescent contributions do not scale with a solid angle subtended by the fluorescing material. Pravdo (1979) concluded that thermal emission must contribute because fluorescence off a surface could not explain so large an equivalent width. However, it can if the direct flux is hidden, and the column hides the emission region from direct view. On the other hand Rothschild et al. (1981) discounted a thermal contribution because of no apparent low temperature continuum. The column can also hide that.

It might at first seem that if there were a larger abundance of Fe, the required $\tau_\perp$ would be lower and the luminosity discrepancy alleviated. But the line emission, the depth of the Fe K_α absorption edge and the lower energy spectrum must be considered together and $\tau_\perp$ lower by a factor of 10 would entail a low energy excess even if the column is cold.

It will be possible with experiments presently envisioned to accurately determine the ratio of the thermal to fluorescent components of the Fe emission features in sources like AM Her and 2A0311-227. The shape and distortion of the fluorescent component would more accurately determine $\tau_\perp$ and then determination of even the average energy of the thermal component would constrain the temperature distribution in the emission region. Such measurements would be possible on other AM Her objects a factor of 10 less intense, which would be below the sensitivity limit of high energy experiments for measuring a shock temperature from the continuum.

ACKNOWLEDGMENTS

We thank Jim Pringle for discussions concerning the nature of the accretion and for pointing out the difficulty of confining nuclear burning to a spot. To D.Q. Lamb we owe appreciation of the virtues, despite the difficulties, of small shock regions. We have also benefited from discussions with Nick White, Andrew King and Peter Serlemitsos.

TABLE 1: OBSERVED FLUXES FROM THE X-RAY BRIGHT POLE

	BAND	NOTATION	10^{-10} ergs $cm^{-2}s^{-1}$	REF. AND NOTE
r	3.5μm - 4500 A	F_r	< 2.6	1,2
u	1150 A - 3400 A	F_u	1.3	3,4
s	0.17 keV - 0.5 keV	F_s	8	5,6a
"	"	"	1.3	6b
"	0.13 keV - 0.28 keV	"	5.9	7
h	0.5 keV - 150 keV	F_h	4.1	8,9

1. Stockman et al. 1977.
2. Priedhorsky et al. 1978. Integral, estimated from spectrum at maximum, includes contribution of red star.
3. Raymond et al. 1979. Integral of component α ν^2.
4. Tanzi et al. 1980.
5. Tuohy et al. 1978. Typical non-eclipse 1977 value.
6. Tuohy et al. 1981. (a) Peak 1978 value. (b) Value during short interval when spectral data was accumulated.
7. Heise et al. 1982. Averaged over variable flux and spectrum.
8. Rothschild et al. 1981. 1977 and 1978 values.
9. Swank and Szkody 1984.

TABLE 2. ESTIMATED LUMINOSITIES OF X-RAY BRIGHT POLE

BAND	ASSUMPTION*	10^{32} ergs s^{-1} d_{100}^{2} **	NOTE
r	$L_r \sim \pi\ d^2\ F_r$	0.8	
u	$L_u \sim \pi\ d^2\ F_u$	0.4	
	$L_u^b \sim \pi\ d^2\ F_u^b$	$0.8\ (\frac{kT}{5eV})^3$	1
s	$L_s \sim \pi\ d^2\ F_s$	2.4	
	$L_s^b \sim \pi\ d^2\ F_{s1}^b$	6	2
	$\sim \pi\ d^2\ F_{s2}^b$	20	3
h	$L_h \sim 2\pi\ d^2\ F_h$	2.5	

* Optically thick surface, normal to line of sight, assumed for r, u, and s. Emissivity independent of angle assumed for h. Superscript b refers to bolometric quantity, corrected for interstellar absorption and limited energy coverage.

** d_{100} = (d/100 pc) for a source distance d.

1. No deviation from the Rayleigh-Jeans spectrum has been reported up to 10 eV.

2. Best blackbody fit for kT = 46 eV, $N_H = 3.2 \times 10^{19}$ cm^{-2} (Heise et al. 1982).

3. kT = 40 eV, $N_H = 2 \times 10^{20}$ cm^{-2} blackbody fit (Tuohy et al. 1978).

REFERENCES

Bai, T. 1979, Solar Phys. 62, 113.

Bai, T., and Ramaty, R. 1978, Ap. J. 219, 705.

Barrett, P.E., and Chanmugam, G. 1984, Ap. J. in press.

Basko, M.M. 1978, Ap. J. 223, 268.

Blackwell, D.E., and Shallis, M.J. 1979, M.N.R.A.S. 186, 673.

Brainerd, J.J., and Lamb, D.Q. 1983, in Cataclysmic Variables and Low Mass Binaries, ed. D.Q. Lamb and J. Patterson, in press.

Chandrasekhar, S. 1958, An Introduction to the Study of Stellar Structure, (New York: Dover) p. 427.

Chanmugam, G., and Wagner, R.L. 1978, Ap. J. 222, 641.

Ferland, G.J., and Truran, J.W. 1980, Ap. J. 240, 608.

Ferland, G.J., and Truran, J.W. 1981, Ap. J. 244, 1022.

Fabbiano, G., Hartmann, L., Raymond, J., Steiner, J., Branduardi-Raymont, G., and Matilsky, T. 1981, Ap. J. 243, 911.

Fireman, E.L. 1974, Ap. J. 187, 57.

Frank, J., King, A.R. and Lasota, J.P. 1982, Univ. of Leicester preprint.

Fujimoto, M.Y. 1982, Ap. J. 257, 767.

Fujimoto, M.Y., and Truran, J.W. 1982, Ap. J. 257, 303.

Hatchett, S., Buff, J., and McCray, R. 1976, Ap. J. 206, 847.

Heise, J., and Brinkman, A.C. 1982, in Galactic X-Ray Sources, ed. P.W. Sanford, P. Laskarides, and J. Salton (New York: Wiley), p. 393.

Heise, J., Kruszewski, A., Chlebowski, T., Mewe, R., Kahn, S., and Seward, F.D. 1982, paper presented at the European Conference on "Very Hot Plasmas in Astrophysics", in Nice, Nov. 1982.

Imamura, J.N., and Durisen, R.H. 1983, Ap. J. 268, 291.

Katz, J.I. 1977, Ap. J. 215, 265.

King, A.R. 1982, in IAU Colloquium No. 72, Cataclysmic Variables and Related Objects, ed. M. Livio and G. Shaviv (Dordrecht:Reidel), p. 181.

King, A.R., and Lasota, J.P. 1979, M.N.R.A.S. 188, 653.

Kuijpers, J., and Pringle, J.E. 1982, Astr. Ap. 114, L4.

Kylafis, N.E. 1978, PH.D. Thesis, University of Illinois at Urbana-Champagne.

Kylafis, N.D., and Lamb, D.Q. 1979, Ap. J. (Letters) 228, L105.

Kylafis, N.D., and Lamb, D.Q. 1982, Ap. J. Suppl. 48, 239.

Lamb, D.Q. 1983, in IAU Colloquium No. 72, Cataclysmic Variables and Related Objects, ed. M. Livio and G. Shaviv (Dordrecht:Reidel), p. 299.

Latham, D.W., Leibert, J. and Steiner, J.E. 1981, Ap. J. 246, 919.

Paczynski, B., and Zytkow, A.N. 1978, Ap. J. 222, 604.

Pagel, B.E.J., and Edmunds, M.G. 1981, Ann. Rev. Astron. Astrophys. 19, 77.

Papaloizou, J.C.B., Pringle, J.E. and MacDonald, J. 1981, M.N.R.A.S. 198, 215.

Patterson, J., Williams, G. and Hiltner, W.A. 1981, Ap. J. 245, 618.

Patterson, J., Beuermann, K., Lamb, D.Q., Fabbiano, G., Raymond, J.C., Swank, J.H., and White, N.E. 1983, Ap. J., in press.

Pravdo, S.H. 1979, X-ray Astronomy, eds. W. Baity and L. Peterson (Oxford: Pergammon Press), p. 169.

Pravdo, S.H., and Smith, B.W. 1979, Ap. J. (Letters) 234, L195.

Priedhorsky, W., Mathews, K., Neugebauer, G., Werner, M., and Krezminski, W., 1978, Ap. J. 226, 397.

Raymond, J.C., and Smith, B.W. 1977, Ap. J. Suppl. 35, 419.

Raymond, J.C., and Smith, B.W. 1979, private communication.

Raymond, J. C., Black, J.H., Davis, R.J., Dupree, A.K., Gursky, H., Hartmann, L., and Matilsky, T.A. 1979, Ap. J. (Letters) 230, L95.

Ross, R.R., and Fabian, A.C. 1980, M.N.R.A.S. 193, 1p.

Rothschild, R.E., et al. 1981, Ap. J. 250, 723.

Schmidt, G.D., Stockman, H.S., and Margon, B. 1981, Ap. J. (Letters) 243, L157.

Serlemitsos, P.J. 1982, in X-ray Astronomy in the 1980's, ed. S.S. Holt, NASA TM 83848, p. 441.

Stockman, H.S., Schmidt, G.D., Angel, J.R.P., Liebert, S., Tapic, S., and Blaver, E.A. 1977, Ap. J. 217, 815.

Storm, E. and Israel, H.I. 1967, Los Alamos Scientific Laboratory Report, LA-3753.

Swank, J.H. 1979, in IAU Colloquium 53, White Dwarfs and Variable Degenerate Stars, ed. H.M. Van Horn and V. Weidemann (Rochester: University of Rochester), p. 135.

Swank, J.H., and Szkody, P. 1984, in preparation.

Tanzi, E.G., Tarengni, M., Treves, A., Howarth, I.D., and Willis, A.J. 1980, Astr. Ap. 83, 270.

Tuohy, I.R., Lamb, F.K., Garmire, G.P. and Mason, K.O. 1978, Ap. J. (Letters) 226, L17.

Tuohy, I.R., Mason, K.O., Garmire, G.P. and Lamb, F.K. 1981, Ap. J. 245, 183.

Weast, G.J., Durisen, R.H., Inamura, J.N., Kylafis, N.D. and Lamb, D.Q. 1979, in IAU Colloquium #53 White Dwarfs and Variable Degenerate Stars, ed. H.M. Van Horn and V. Weidemann (Rochester: University of Rochester, p. 140).

White, N.E. 1981, Ap. J. (Letters) 244, L85; 248, L87.

Withbroe, G.L. 1971, in The Menzel Symposium, NBS Special Pub. 353, ed. K.B. Gebbie (Washington: U.S. Government Printing Office), p. 127.

Young, P., Schneider, D.P. and Schectman, S.A. 1981, Ap. J. 245, 1043.

FIGURE CAPTIONS

Figure 1 - The accretion column used in the calculations.

Figure 2 (lower) - Total equivalent width of thermal plus fluorescent Fe K_α emission versus the Thomson optical depth across a diameter of the accretion column just above the shock. Results are shown for a "cold" column (squares) in which only H and He are assumed ionized and for a "partially ionized" column (circles) for a 30 keV bremsstrahlung emission spectrum. Filled symbols denote a continuum approximating the data; F denotes that it is too flat, S too steep. Filled symbols enclosed in open ones are the observed equivalent widths when 10% of the emitted X-rays are assumed to be viewed directly out the sides of a shock region of finite height. Triangles are results assuming a lower temperature component (5 keV) in the emission spectrum with the relative fraction indicated as a superscript.

(upper) - Ratio of thermal to fluorescent components. Bars denote a range possible for acceptable models.

Figure 3 - Continua for selected emission spectra for $\tau_\perp$ too small (a), in an acceptable range (b) and too large (c). The heavy line (——) indicates the observed spectrum (averaged over noneclipse phases). (a) and (b) show results for 2 temperature models (——) and spectra generated in spherically symmetric shock models (-·-·-). The former are, in (a) for $\tau_\perp = 0.15$, $x = 0.5$ and in (b) for $\tau_\perp = 0.2$, $x = 0.5$ and $\tau_\perp$ 0.7, $x = 0.2$. The latter are, in (a) for $M_1 = 1.2$, $L/fL_E = 0.025$, $L_{BB} = 4 \times 10^{37}$, $\tau_\perp = 0.15$ and for $M_1 = 1.0$, $L/fL_E = 0.014$, $L_{BB} = 4 \times$

10^{37}, $\tau_\perp = 0.1$, both for a cold column; in (b) for $M_1 = 1.3$, $L/fL_E = 0.03$, $L_{BB} = 7 \times 10^{37}$, and $\tau_\perp = 0.3$ for both cold (lower) and partially ionized columns (upper). In (c) the albedo is also shown for 30 keV bremsstrahlung. The two $\tau_\perp = 3$ curves are for a cold (lower) and partially ionized column (upper).

Figure 4 - (a) "Light" curves as a function of angle between a cold accretion column and observer for the 1-4 keV and the 4-60 keV flux with the hardness ratio. (b) Spectra that would be observed averaged over 20^o angles for a 2 temperature emission spectrum and a partially ionized column. The same trend is seen as for a cold column.

Figure 5(a) - Gravitational power available implied by $\tau_\perp = 0.2$, 0.3 and 0.7 for column cross section $f = 2 \times 10^{-3}$ of white dwarf surface area and $\tau_\perp = 0.3$ for $f = 2 \times 10^{-4}$. (---) L_G corresponding to a high accretion rate range in which steady nuclear burning could occur if scaled to the fraction $f = 2 \times 10^{-3}$ of the surface. The horizontal shaded areas indicate $L_h + L_r + L_s^b$ for a distance between 75 and 100 pc. The lower range is for $L_{s1}^b = 6 \times 10^{32}\ d_{100}^2$ and the upper for $L_{s2}^b = 2 \times 10^{33}\ d_{100}^2$ in ergs s^{-1}. (b) L_G as a function of white dwarf mass if f is determined from L_s^b, assuming a face-on blackbody emission surface and $\tau_\perp = 0.3$. Solutions for which $L_h + L_r + L_s^b = L_G$ are indicated.

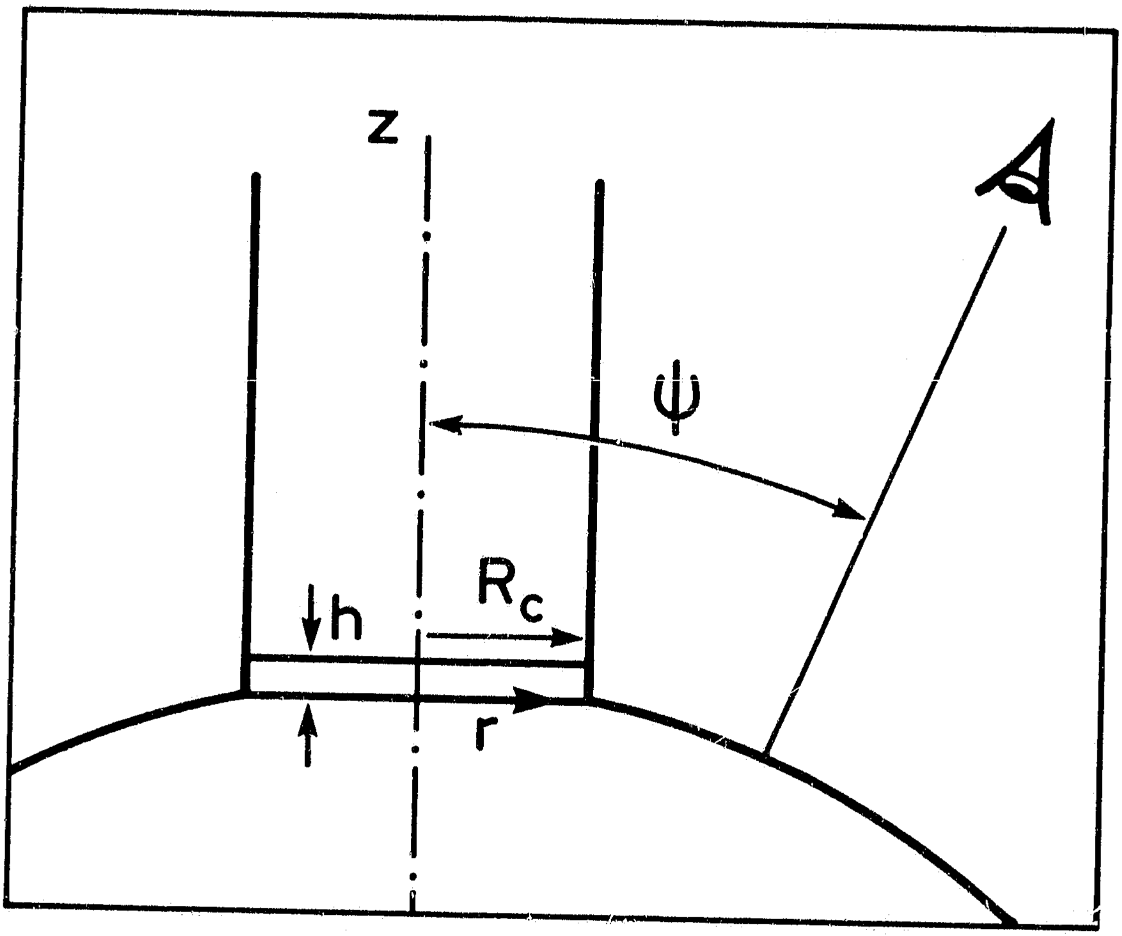
z
ψ
h
R_c
r

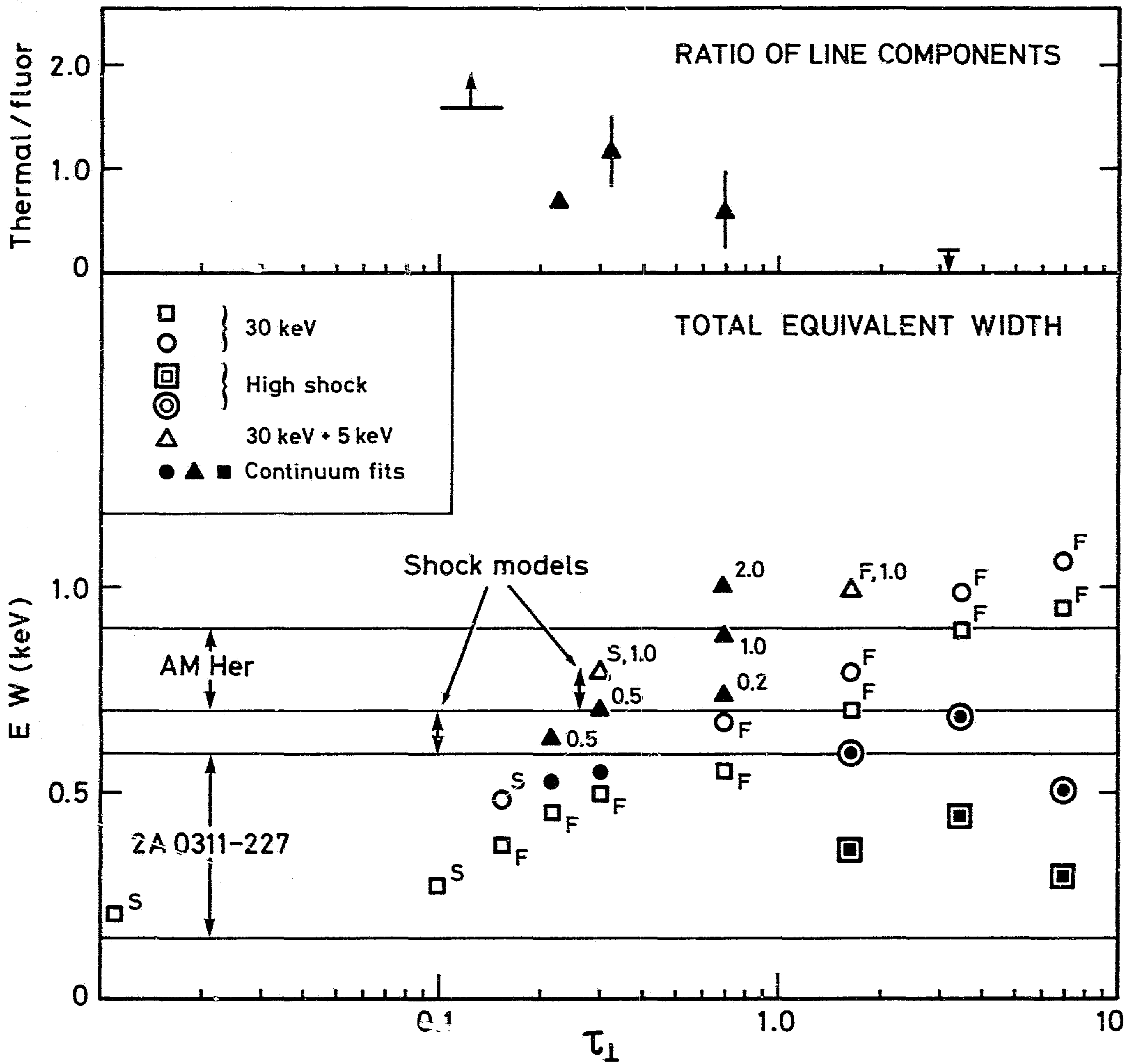

RATIO OF LINE COMPONENTS
Thermal / fluor
2.0
1.0
0
TOTAL EQUIVALENT WIDTH
30 keV
High shock
30 keV + 5 keV
Continuum fits
Shock models
AM Her
2A 0311-227
E W (keV)
1.0
0.5
0
0.1
1.0
10
$\tau_{\perp}$

ORIGINAL PAGE IS
OF POOR QUALITY

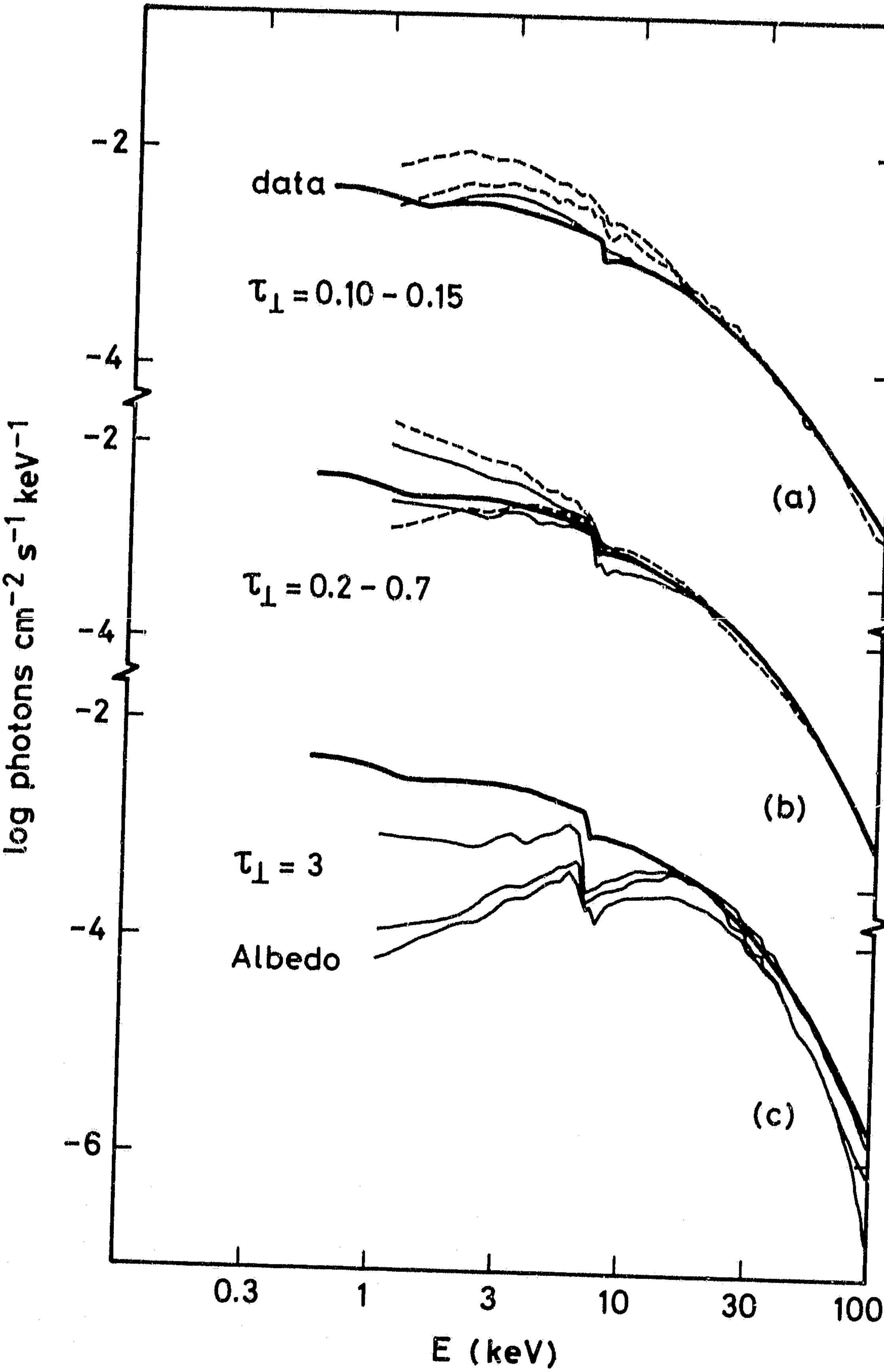

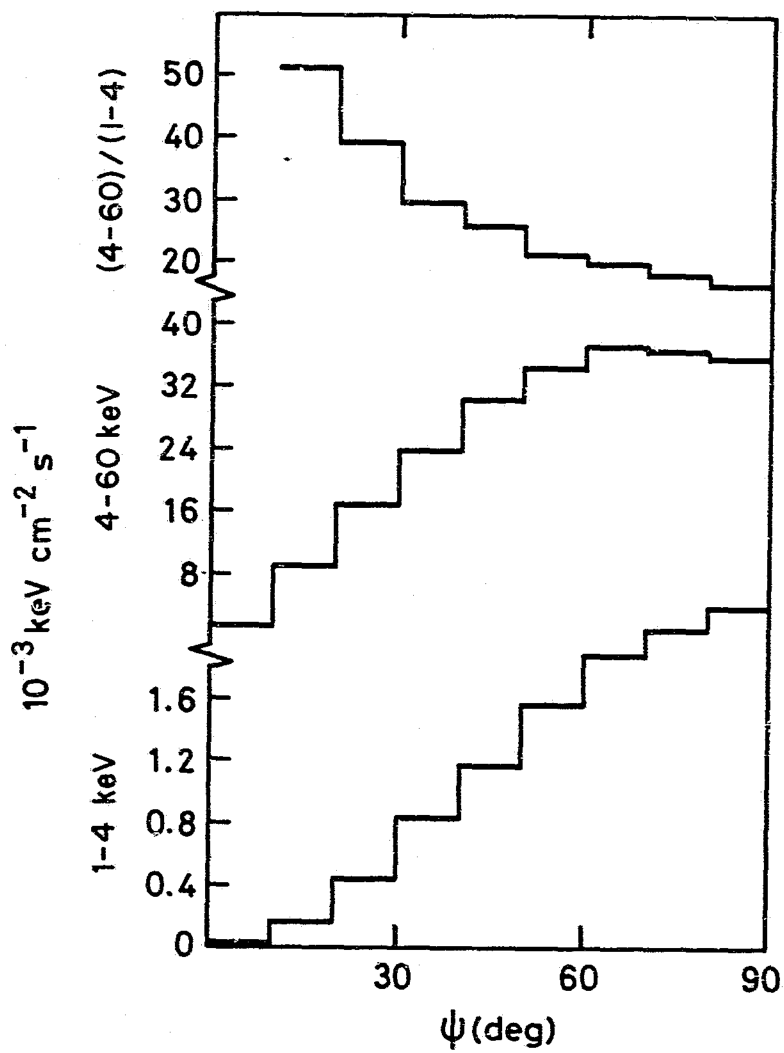
10^-3 keV cm^-2 s^-1
(4-60)/(1-4)
4-60 keV
1-4 keV
50
40
30
20
40
32
24
16
8
1.6
1.2
0.8
0.4
0
30
60
90
ψ (deg)

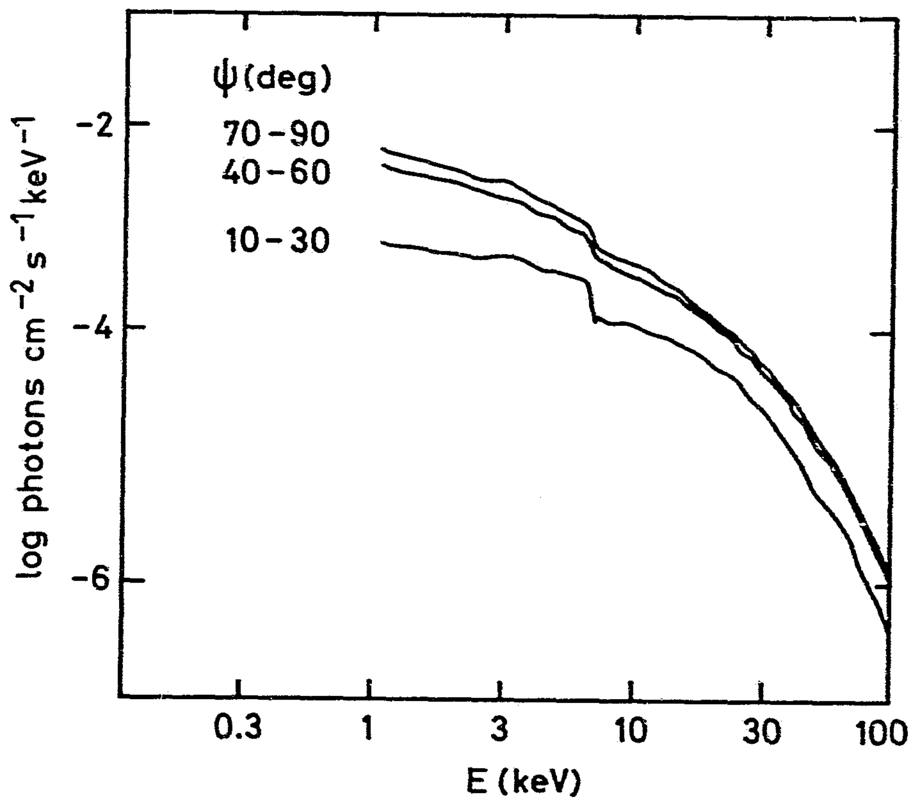
log photons cm^-2 s^-1 keV^-1
ψ (deg)
70-90
40-60
10-30
-2
-4
-6
0.3
1
3
10
30
100
E (keV)

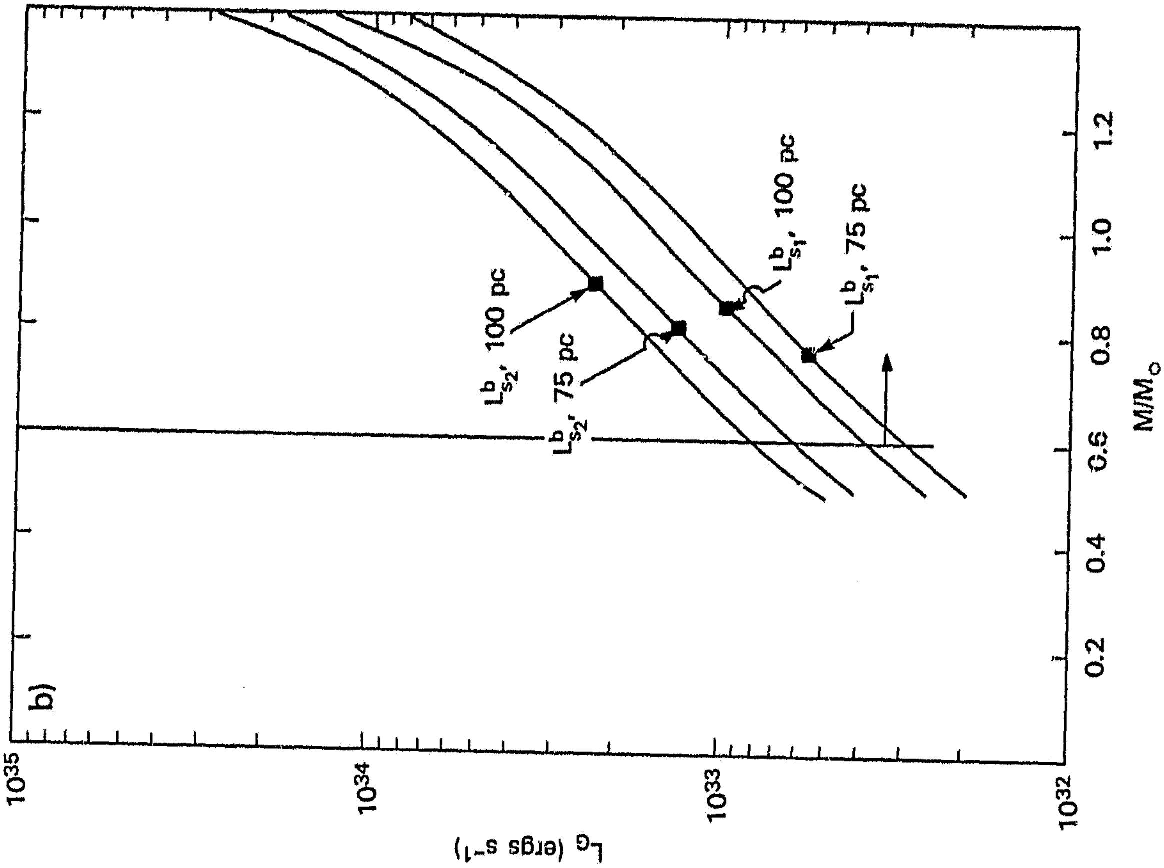
b)
L_G (ergs s^{-1})
10^{35}
10^{34}
10^{33}
10^{32}
M/M$_\odot$
0.2
0.4
0.6
0.8
1.0
1.2
$L^b_{s_2}$, 100 pc
$L^b_{s_2}$, 75 pc
$L^b_{s_1}$, 100 pc
$L^b_{s_1}$, 75 pc

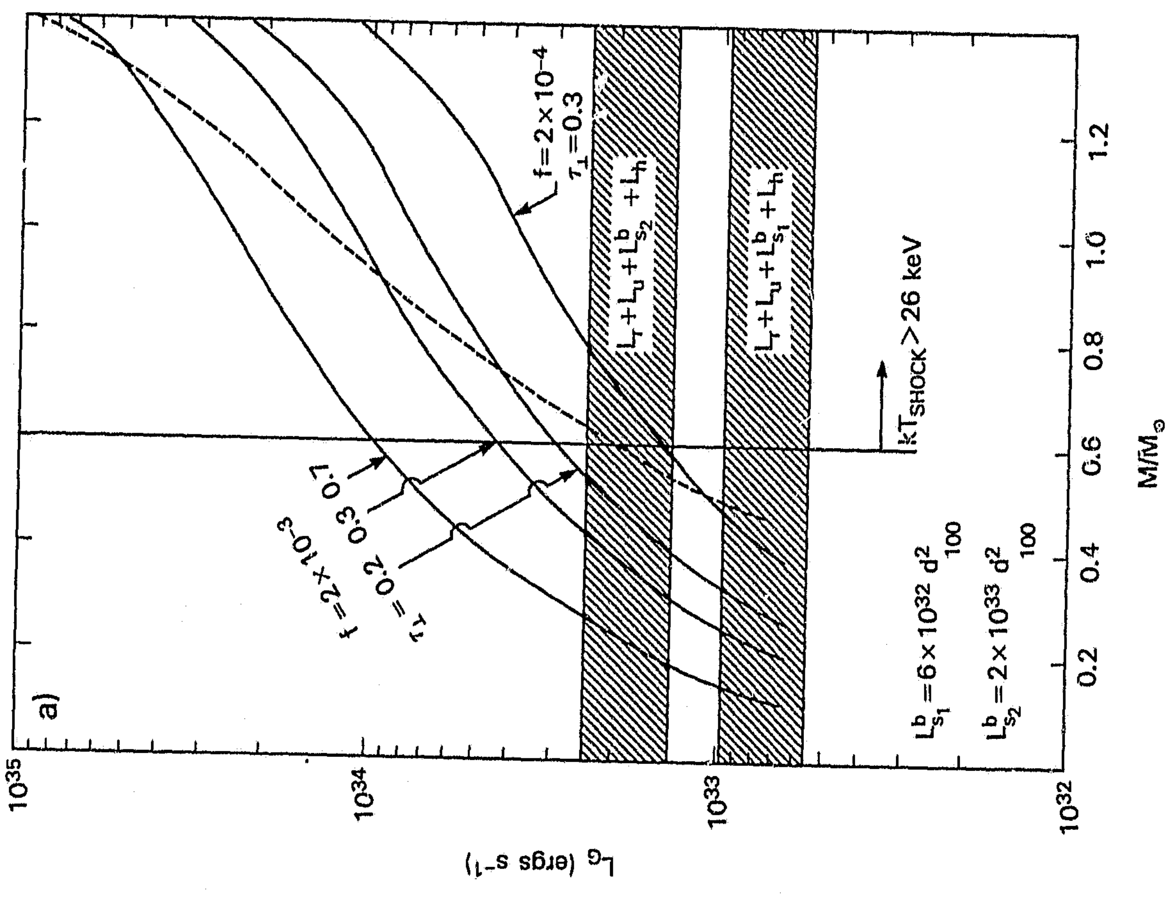
a)
L_G (ergs s^{-1})
10^{35}
10^{34}
10^{33}
10^{32}
M/M$_\odot$
0.2
0.4
0.6
0.8
1.0
1.2
$f = 2\times10^{-3}$
$\tau_\perp = 0.2$ 0.3 0.7
$f = 2\times10^{-4}$
$\tau_\perp = 0.3$
$L_r + L_u + L^b_{s_2} + L_h$
$L_r + L_u + L^b_{s_1} + L_h$
$kT_{SHOCK} > 26$ keV
$L^b_{s_1} = 6\times10^{32}\ d^2_{100}$
$L^b_{s_2} = 2\times10^{33}\ d^2_{100}$

ADDRESS OF AUTHORS

A.C. FABIAN, Institute of Astronomy, Madingley Road, Cambridge CB3 0HA, ENGLAND

J.H. SWANK, Code 661, Laboratory for High Energy Astrophysics, NASA/Goddard Space Flight Center, Greenbelt, MD 20771

R.R. ROSS, Physics Department, College of the Holy Cross, Worcester, MA 01610